ISSN 0015-4628, Fluid Dynamics, 2018, Vol. 53, No. 6, pp. 750–761. © Pleiades Publishing, Ltd., 2018.
Original Russian Text © A.V. Bazilevskii, V.A. Kalinichenko, A.N. Rozhkov, 2018, published in Izvestiya Rossiiskoi Akademii Nauk, Mekhanika Zhidkosti i Gaza, 2018, No. 6, pp. 30–42.

Effect of Fluid Viscosity on the Faraday Surface Waves

A. V. Bazilevskii[1]*, V. A. Kalinichenko[1,2], and A. N. Rozhkov[1]*****

[1] *Ishlinsky Institute for Problems in Mechanics of the Russian Academy of Sciences, Moscow*

[2] *Bauman Moscow State Technical University, Moscow*

Received June 4, 2018

Abstract—The comprehensive experimental analysis of the fluid viscosity effect on the standing gravity waves excited at parametric resonance is carried out. The viscous effects on the frequency range of excitement of the second wave mode, its resonance dependences, and the processes of damping and approaching the steady-state regime are quantitatively estimated by varying the viscosity over a wide range. It is found that the waves are regularized without breaking when the kinematic viscosity of the working medium becomes higher than a threshold value. A mechanism of viscous regularization of wave motion is suggested. In accordance with this mechanism, the effects observed experimentally relate to the presence of the shortwave cutoff domain in which viscous dissipation becomes the dominant factor and the shortwave perturbations responsible for breaking the standing wave are suppressed.

Key words: regular, irregular, and breaking Faraday waves, fluid viscosity, dissipation effects, damping coefficient.

DOI: 10.1134/S0015462818060150

The set of the experiment [1], namely, a vessel with fluid oscillating in the vertical direction is considered, unifies many studies on parametric resonance in fluid with the free surface. Under the resonance conditions, the wave motions of fluid are observed in the form of standing surface waves whose frequency is multiple to half the vessel frequency, i.e., the Faraday waves. The fluid viscosity is responsible for narrowing the frequency range of excitation of surface waves, i.e. the vessel oscillation amplitude must be greater that a certain threshold value [2, 3]. Under the experimental conditions, the dissipative wave losses can be quantitatively estimated in terms of the damping coefficient, the threshold amplitude, and the parametric oscillation breakdown frequency [4].

The height of the excited Faraday waves depends on the vessel oscillation frequency and can increase when the frequency varies gradually. As shown in [5], as the wave height increases, the nature of oscillations of the free fluid surface changes radically, namely, the regular waves transform into breaking waves characterized by jet ejections and droplet separations on the wave crest. This wave breakdown pattern can be observed not only for the Faraday waves but also for the steading surface gravity waves excited by wave-generators on the end-face walls of a rectangular vessel [6] and under harmonic oscillations of the vessel in the horizontal direction [7]. We note that water was used as the working fluid in these studies and no experiments on the investigation of the effect of viscosity of the medium on transition to breaking waves were carried out.

The effect of viscosity on the free capillary-gravity [8–10] and gravity waves [11] was taken theoretically into account by separating the motion of fluid onto the potential and vortex parts. In the linear formulation this makes it possible to obtain the complex dispersion relation.

The aim of the present study is to investigate experimentally the effect of fluid viscosity on breaking standing gravity surface Faraday waves. In [12] the authors showed that increase in the viscosity by two orders leads to wave regularization, but the effect of intermediate values of the viscosity was not considered. In what follows, we will discuss the results of experiments in which the fluid viscosity changes from 1 to 86 cSt. The theme of the investigations relates to the solution of practical problems

*E-mail: baz@ipmnet.ru.
**E-mail: kalin@ipmnet.ru.
***E-mail: rozhkov@ipmnet.ru.

Table 1

ρ, g/cm^3	ν, cSt	$\Delta\Omega$, s^{-1}	Γ	δ
Water				
1.00	1	0	0.21	0.09
Vegetable oil–kerosine solution				
0.89	25.35	0.175	0.24	0.262
0.90	31.51	0.415	0.272	0.295
0.90	39.52	0.465	0.280	0.348
0.91	46.33	0.775	0.297	0.403
0.92	56.42	0.975	0.326	0.441
0.93	63.34	1.292	0.310	0.543
Aqueous sugar solution				
1.21	9.03	0.075	0.215	0.176
1.23	16.24	0.195	0.261	0.255
1.25	28.96	0.515	0.267	0.341
1.28	48.30	0.635	0.309	0.368
1.30	85.97	1.292	0.230	0.439

of aerospace techniques, petroleum product transfer by sea and ground transports, and suppression of oscillations of fluid with the free surface in the form of standing waves [3, 13].

1. SET OF THE EXPERIMENT

Similarly to [12], for studying the effect of viscosity on intense fluid oscillations, we have used the regime of parametric excitation of the second mode ($n = 2$) of standing gravity waves on the free surface of a fluid of depth $h = 15$ cm located in the rectangular vessel made of plexiglass of length $L = 50$ cm, width $W = 4$ cm, and height 50 cm. Its vertical harmonic oscillations at a frequency Ω and with an amplitude s were provided by an electromechanical vibration table.

The two-dimensional wave motions were investigated in the regime of basic Faraday resonance [5, 12]. In this regime the vessel oscillation frequency Ω is higher than the frequency ω of the excited waves by two times. The frequency Ω was varied over the range 18–24 s^{-1} when the amplitude was fixed $s = 0.75$ cm. This ensured variation in the steepness $\Gamma = H/\lambda$ on the interval 0.004–0.66 at the wave length $\lambda = 50$ cm (here, H is the wave height defined as the distance between the trough and the crest of a wave). The range of variation in the overloading $\varepsilon = s\Omega^2/g$ is estimated from 0.24 to 0.44.

In the experiments we used degasified tap water, mixtures of vegetable oil and kerosine, and aqueous sugar solutions. Variation in the fluid viscosity was implemented by adding kerosene in oil or water in 63% sugar solution. The dynamic viscosity of the solutions thus obtained was measured using the HAAKE RS-1 rheometer and their density by an areometer. The surface tensions borrowed from the literature are equal to $\sigma = 73$, 40, and 80 dyne/cm for water, vegetable oil, and 63% sugar solution, respectively. The measurements and experiments were carried out at temperature of 20–21°C. In Table 1 we have presented the values of the density ρ and the kinematic viscosity ν of the liquids used in the experiments.

The Reynolds number $\mathrm{Re} = U_0\lambda/\nu$ determined from the maximum velocity $U_0 = \Omega H/4$ and the wave length $\lambda = 50$ cm varied within the limits from 10^3 to 10^6.

The waves were recorded by video using the DIMAGE Z2 and Canon PowerShot SX50HS cameras at the speed of 30 and 120 frames per second. The ImageJ program was used for successive processing of the video-tapings.

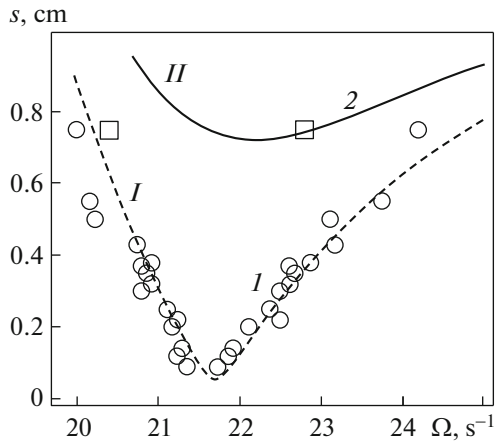

Fig. 1. Instability domains of the second wave mode: *1* and *2* correspond to water and oil, respectively.

The experimental value of the damping coefficient b was estimated using the methods described in [14]: the vibration table was switched off after establishing steady-state fluid oscillations at one of the resonance frequencies Ω and the process of damping the second wave mode was taped by video after full stopping of the vessel.

According to the video recording data, the accuracy of measurements of the displacement of the free fluid surface from the equilibrium position was 0.1 cm. The quantity b was determined as follows: $b = T^{-1}\ln(H_m/H_{m+1})$, where $T = 2\pi/\omega$ is the wave period and H_m and H_{m+1} are the wave heights taken in the oscillation period. The damping rate $\delta = bT$ was used as the dimensionless characteristic of the dissipative fluid properties.

Under the experimental conditions the Faraday waves are similar to free surface waves whose frequency is equal to $\omega_0 = (gk\tanh kh)^{1/2} = 10.85\ \text{s}^{-1}$, where g is the gravity acceleration and $k = 2\pi/\lambda$ is the wavenumber. The damping coefficients obtained experimentally are $b_{\text{exp}} < 1\ \text{c}^{-1}$ for all the fluids. Since $\omega_0/b_{\text{exp}} \sim 10$, the media under consideration can be related to low-viscosity ones in the wave process considered.

The theoretical model [15] was used to interpret the experimental data on wave excitation.

2. RESULTS AND DISCUSSION

First of all, the frequency range of excitation of the surface Faraday waves was investigated. In Fig. 1 we have reproduced the instability domains of the free surface of water and oil. From these data it follows that the frequency range of excitation narrows significantly for the higher-viscosity fluid. Moreover, there is a threshold value s^* of the vessel oscillation amplitude associated with viscosity which is equal to 0.04 cm for water and 0.7 cm for oil. This fact determined the choice of the quantity $s = 0.75$ cm which guarantees experimental excitation of the second mode on the surface of both water and oil and 63% sugar solution.

Curves I and II are the calculated theoretical boundaries of the instability zone [15] determined by the inequalities

$$1 - \sqrt{(\varepsilon/2)^2 - 16b^2/\Omega^2} < 2\omega/\Omega < 1 + \sqrt{(\varepsilon/2)^2 - 16b^2/\Omega^2}.$$

The Faraday waves observed on the water surface can be divided into three categories: regular, irregular, and breaking waves [5].

The regular waves are the waves whose profile possesses the temporal periodicity and the spatial symmetry about the vertical passed through the wave crests.

The waves for which the temporal periodicity and spatial symmetry are violated but the entire volume of oscillating fluid still conserves connectedness were classified as irregular waves.

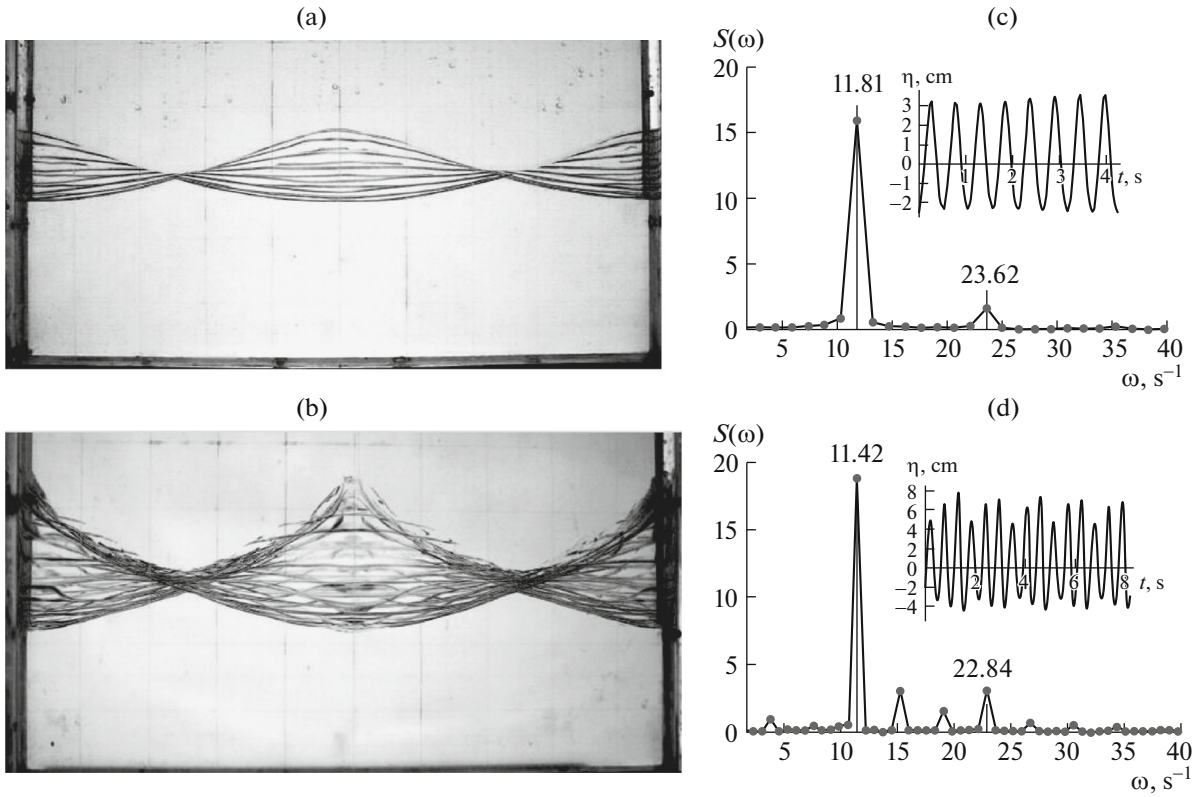

Fig. 2. Envelopes of the free water surface in the case of the regular and irregular waves (a and b, respectively); the corresponding wave frequencies and heights: $\Omega = 23.62$ and 22.85 s^{-1} and $H = 5.1$ and 10.5 cm; spectra and chronograms (in inserts) of the displacement of fluid at the center of vessel for $\Omega = 23.62$ and 22.85 s^{-1}.

The waves in which individual liquid droplets or jets are separated from the free surface were related to breaking Faraday waves. These waves are characterized by transition from simply to multiply connected free surface.

In Figs. 2a and 2b we have reproduced examples of the envelopes of free surface for the regular and irregular waves. The envelopes are the result of superposition of 60–70 frames at the speed of 30 frames per second. This corresponds to the time interval of approximately 5 oscillation periods. The chronograms and the amplitude-frequency spectra $S(\omega)$ of the displacement of free fluid surface at the center of vessel were obtained from the video-taping data (see Figs. 2c and 2d).

We can see that the regular wave is nonlinear as a result of asymmetry of the wave profile (Fig. 2a) and its spectrum (Fig. 2c) has two peaks at the frequencies 11.81 and 23.62 s^{-1} corresponding to the main and second harmonics.

In addition to the main and second harmonics (11.42 and 22.84 s^{-1}, respectively), the spectrum of the irregular wave (Figs. 2b and 2d) has peaks at the frequencies 3.77, 15.34, 19.10, 26.63, 30.49, and 34.35 s^{-1}.

In Fig. 3 we have reproduced breaking waves corresponding to the frequencies $\Omega = 22.07$ and 19.51 s^{-1} (a and b, respectively). If in the case (a) the wave breakdown is manifested in the form of jet ejections from the wave crest with separation of individual droplets, then for (b) lateral ejections and separation of considerable fluid fragments are also characteristic.

The waves observed on the surfaces of oil and sugar solution of the maximum viscosity ($\nu = 63.34$ and 85.97 cSt) are regular over the entire frequency range of parametric excitation. In Fig. 4 we have reproduced the shape of the free surface obtained by means of superposing ten successive profiles of the maximum development of the wave mode for oil and sugar (a and b, respectively).

In Fig. 5 we have reproduced the envelopes of the free surface, the frequency spectra, and the chronograms of the surface displacement at the center of vessel for two frequencies in the case of oil. The observed waves (a and b) are nonlinear and two peaks corresponding to the first and second

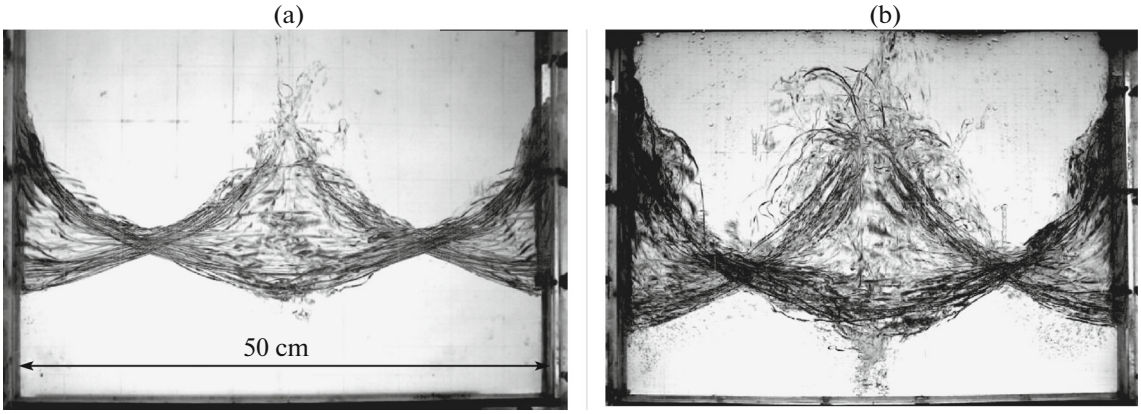

Fig. 3. Breaking waves on the free water surface: *a* and *b* correspond to $\Omega = 22.07$ and 19.51 s^{-1} and $H = 12.6$ and 19.5 cm; the shooting speed is equal to 30 frames per second; the envelopes are obtained by superposition of 100 frames (seven wave periods).

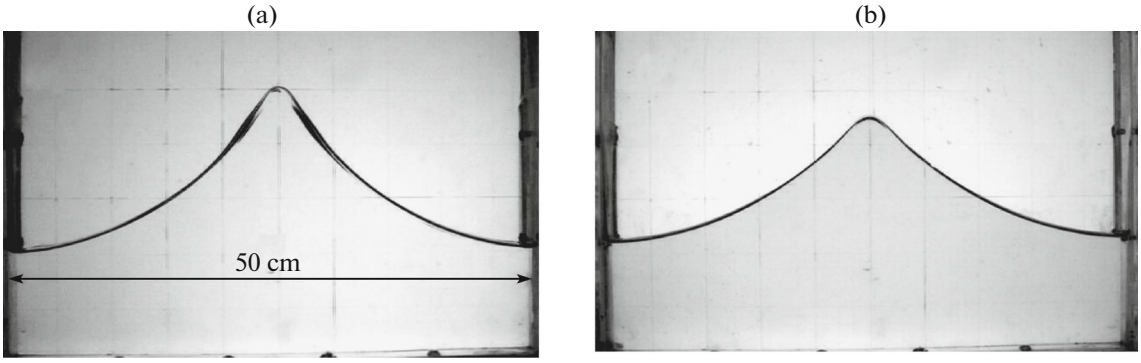

Fig. 4. Regular waves on the surfaces of vegetable oil of the viscosity $\nu = 63.34$ cSt (*a*) and of aqueous sugar solution with $\nu = 85.97$ cSt (*b*); the excitation frequencies $\Omega = 19.69$ and 20.40 s^{-1} and the wave heights $H = 14.7$ and 10.9 cm, respectively.

harmonics can be seen on the spectra (*c* and *d*). The wave heights (*a* and *b*) are commensurable with the corresponding quantities for the irregular and breaking waves on the water surface (see Figs. 2b and 3a); however, there are no any signs of formation of jets or separation of droplets, as in the case of water.

In Fig. 6a we have reproduced the resonance dependences of the steady-state wave height $H(\Omega)$ as a function of the vessel oscillation frequency as the integral wave characteristic. We can see that the wave height increases monotonically with decrease in Ω to a certain frequency corresponding to the oscillation breakdown. This occurs on the surfaces of all fluids considered.

For water (*1*) the regular and irregular (breaking) waves can be observed over the frequency ranges *I* and *II*, whereas the waves on the surface of oil and sugar solution (of maximum viscosity) remain regular over the entire frequency range of excitation of the second wave mode (see data *2* and *3* in Fig. 6a).

We note the shift $\Delta\Omega$ of the resonance dependences for oil (*2*) and sugar solution (*3*) to the low-frequency domain. This is associated with decrease in the eigenfrequency and narrowing of the resonance zones due to increase in the viscosity of the working fluids as compared with water (Fig. 6b and Table 1). As the viscosities of the oil and sugar solutions decrease, the corresponding resonance dependences are displaced to curve *1* for water (Fig. 6a).

Decrease in the viscosity affects not only the frequency shift $\Delta\Omega$ but also changes qualitatively the nature of fluid oscillations. For pure oil ($\nu = 63.34$ cSt) and its mixture with kerosine of viscosity 56.42 cSt, as well as for the sugar solution of maximum viscosity $\nu = 85.97$ cSt, the waves observed are regular at all the frequencies of the dependence $H(\Omega)$, i.e., the limiting steepness is determined by only the breakdown frequency. For oil-kerosine mixtures with $\nu = 46.33$, 39.52, and 31.51 cSt and aqueous sugar solution with $\nu = 48.30$ and 28.96 cSt at a certain Ω the standing wave becomes irregular in

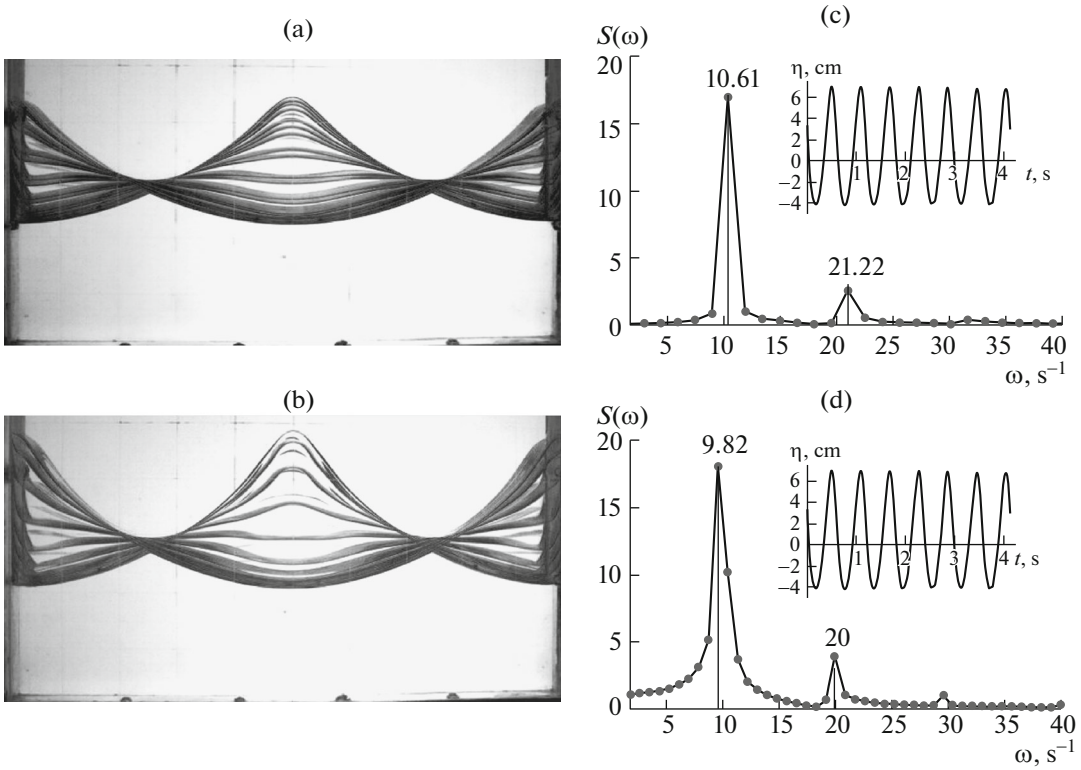

Fig. 5. Envelopes of regular oscillations of the free surface of oil ($\nu = 63.34$ cSt): *a* and *b* correspond to $\Omega = 21.22$ and 19.64 s^{-1} and $H = 11$ and 15 cm, respectively. The corresponding frequency spectra and chronograms (in inserts) of the displacement of fluid surface at the center of vessel (*c* and *d*, respectively).

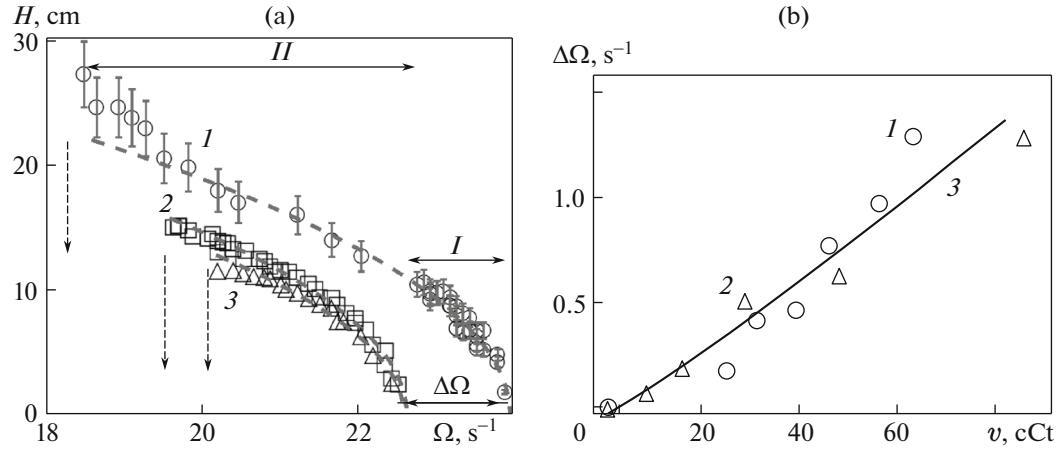

Fig. 6. Resonance dependences $H(\Omega)$ (*a*): *1, 2*, and *3* correspond to water, oil ($\nu = 63.34$ cSt), and aqueous sugar solution ($\nu = 85.97$ cSt), respectively; *I* and *II* correspond to the range of excitation of the regular, irregular, and breaking waves on water; broken arrows correspond to the oscillation breakdown. Frequency shift $\Delta\Omega$ as a function of the viscosity ν of the working medium (*b*): *1* corresponds to the oil-kerosine mixture, *2* to the aqueous sugar solution, and *3* to the approximating curve $\Delta\Omega = 0.04 + 0.01\nu^{1.1}$.

conserving connectedness of fluid. In the case of oil-kerosine mixtures with $\nu = 25.35$ cSt and aqueous sugar solution with $\nu = 16.24$ cSt characteristic indications of wave breaking can be observed, namely, these are jet ejections from the wave crest with separation of droplets and considerable fluid fragments.

Thus, the results of our experiments on excitation of standing waves on the free surface of a viscous fluid make it possible to conclude the following. If the vessel oscillation frequency Ω decreases along the resonance curve $H(\Omega)$ (wave height increases), then only the regular waves can be observed when

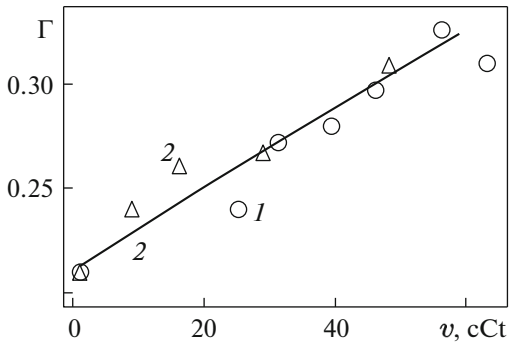

Fig. 7. Limiting steepness $\Gamma = H/\lambda$ of the regular wave as a function of the fluid viscosity ν: *1* corresponds to the oil-kerosine mixture, *2* to the aqueous sugar solution, and *3* to the approximating curve $\Gamma = 0.21 + 0.002\nu$.

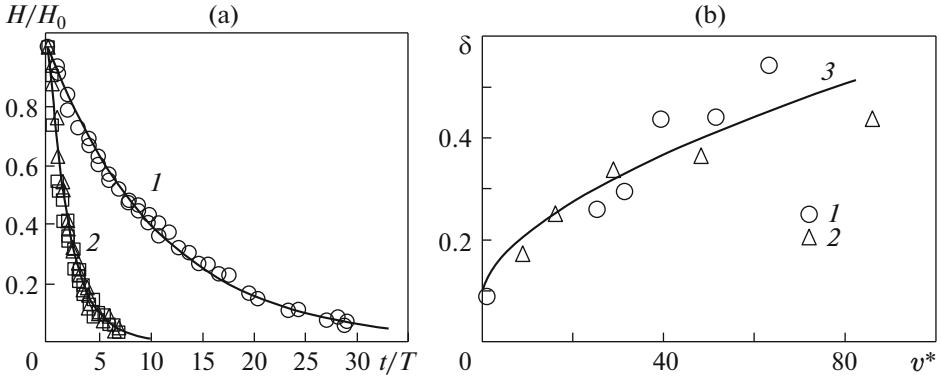

Fig. 8. Damping of the second wave mode (*a*) on the free surface of water (*1*) and oil (sugar solution) (*2*); T is the wave period. The damping rate of the second wave mode (*b*) as a function of the kinematic viscosity ν^* normalized by the water viscosity: *1* corresponds to the oil-kerosine mixture, *2* to the aqueous sugar solution, and *3* to the approximating curve $\delta = 0.09 + 0.04\sqrt{\nu}$.

$\nu > 50$ cSt. When $\nu < 20$ cSt the fluid behaves similarly to water for which the regular, irregular, and breaking Faraday waves are characteristic. The intermediate interval of the fluid viscosity $20 < \nu < 50$ cSt ensures excitation of the regular and irregular waves without signs of breaking.

An analysis of the resonance dependences makes it possible also to estimate the effect of the fluid viscosity on the limiting height of the regular wave (Table 1). In Fig. 7 we have reproduced the experimental dependence of the limiting wave steepness $\Gamma = H/\lambda$ as a function of the kinematic fluid viscosity ν. If for water $\Gamma = 0.21$, then, as the viscosity of the medium increases, the limiting steepness grows monotonically and reaches $\Gamma = 0.326$ for $\nu = 56.42$ cSt.

The process of damping of the second wave mode is investigated for fluids used in the experiments and the damping rate δ is estimated in varying the initial wave height H_0 from 7 to 12 cm. In the case of water $\delta = 0.092$, whereas for oil and sugar solution of the maximum viscosity we obtained similar values $\delta = 0.495$ and 0.510. Thus, in the case of vegetable oil and sugar solution ($\nu = 63.34$ and 85.97 cSt, respectively) the damping rate increases by five times as compared with water (Fig. 8a).

In Fig. 8b we have reproduced the damping rate δ as a function of the fluid viscosity ν. We can see that the damping rate increases monotonically with the viscosity. In Table 1 we have also given the values of the damping rate δ.

In Fig. 9 we have reproduced the data on establishing the steady-state oscillation regime for water and oil. In the case of both water (*1*) and oil (*2*) the wave height reaches the steady-state value H_{st} approximately in the same time, namely, in $40 - 50$ periods. However, if for oil this process occurs gradually, then damped re-oscillations about the steady-state value with the maximum initial amplitude of oscillations of the order of $0.4H_{st}$ are characteristic of the waves on the water surface.

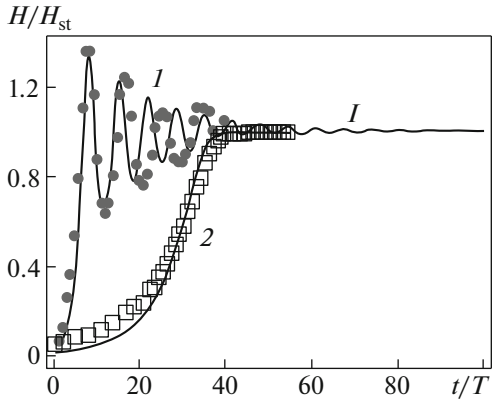

Fig. 9. Process of tending the oscillations to the steady-state regime: *1* corresponds to water, $\Omega = 23.36\ \mathrm{s}^{-1}$, and $H_{st} = 6.8$ cm; *2* corresponds to vegetable oil, $\Omega = 20.94\ \mathrm{s}^{-1}$, and $H_{st} = 11.6$ cm; curve *I* corresponds to the numerical solution of the system (2.1) for $H_0 = 0.1$ cm and $\theta_0 = 0$.

On the basis of the theoretical model [15] the process of establishing the steady-state oscillations can be described by the following system of equations for the height $H(t)$ and the slow phase $\theta(t)$ of the wave:

$$\frac{dH}{dt} = -bH + \frac{\varepsilon}{2\Omega}\omega^2 H \sin 2\theta,$$

$$\frac{d\theta}{dt} = \Delta + \frac{\varepsilon}{2\Omega}\omega^2 \cos 2\theta - \beta\frac{H^2}{4}\omega k^2,$$

$$\beta = \frac{1}{64}\tanh^{-4} kh \left(2\tanh^6 kh + 3\tanh^4 kh + 12\tanh^2 kh - 9\right),$$

$$\psi = \frac{\Omega t}{2} + \theta(t), \quad \Delta = \omega - \frac{\Omega}{2}, \tag{2.1}$$

where ψ is the phase of the wave.

The numerical solution of this system shown in Fig. 9 by curves I describes the experimental data with sufficient accuracy.

The data given in Figs. 1–9 characterize the effects of fluid viscosity on the process of parametric excitation of standing surface gravity waves, namely, the frequency range of excitation of the second wave mode, its resonance dependences, the processes of damping and tending to the steady-state regime. The question of viscous regularization of irregular and breaking waves remains open. With regard to this fact, in what follows we will consider the effects of fluid viscosity on the dynamics of irregular and breaking waves.

For water the transition from irregular to breaking waves takes place when the steepness $\Gamma > 0.22$. In Fig. 10 we have reproduced the sequence of frames showing the generation, development, and collapse of the cavity in the stage of formation of the crest in the central part of the vessel. As a result of trough-crest transition, the central part of fluid is displaced upward and small-scale perturbations of dimensions not greater than 5 cm can be seen on the wave profile in the interval $0.944 - 0.984$ s. A completely formed cavity can be observed in the middle of the wave profile at $t = 1.016$ s. The successive collapse of the cavity ($t \geq 1.040$ s) leads to jet ejection with separation of droplets.

When $\nu > 50$ cSt the wave profiles are absolutely smooth on the surface of vegetable oil and sugar solutions over the entire range of the steepness Γ. As an example, in Fig. 11 we have reproduced the sequence of wave profiles on the oil surface during half the wave period. We can see that the wave is nonlinear but regular, its profile is asymmetric without any small-scale perturbations and signs of collapse.

The only reason of difference between the wave patterns in Figs. 10 and 11 is the viscosity of working fluid. Increase in the viscosity of oscillating fluid to 63.34 cSt leads to total suppression of the collapse process and regularization of standing wave: small-scale perturbations leading to formation of collapsing cavity disappear. We note that the observed regularities are determined but only the fluid

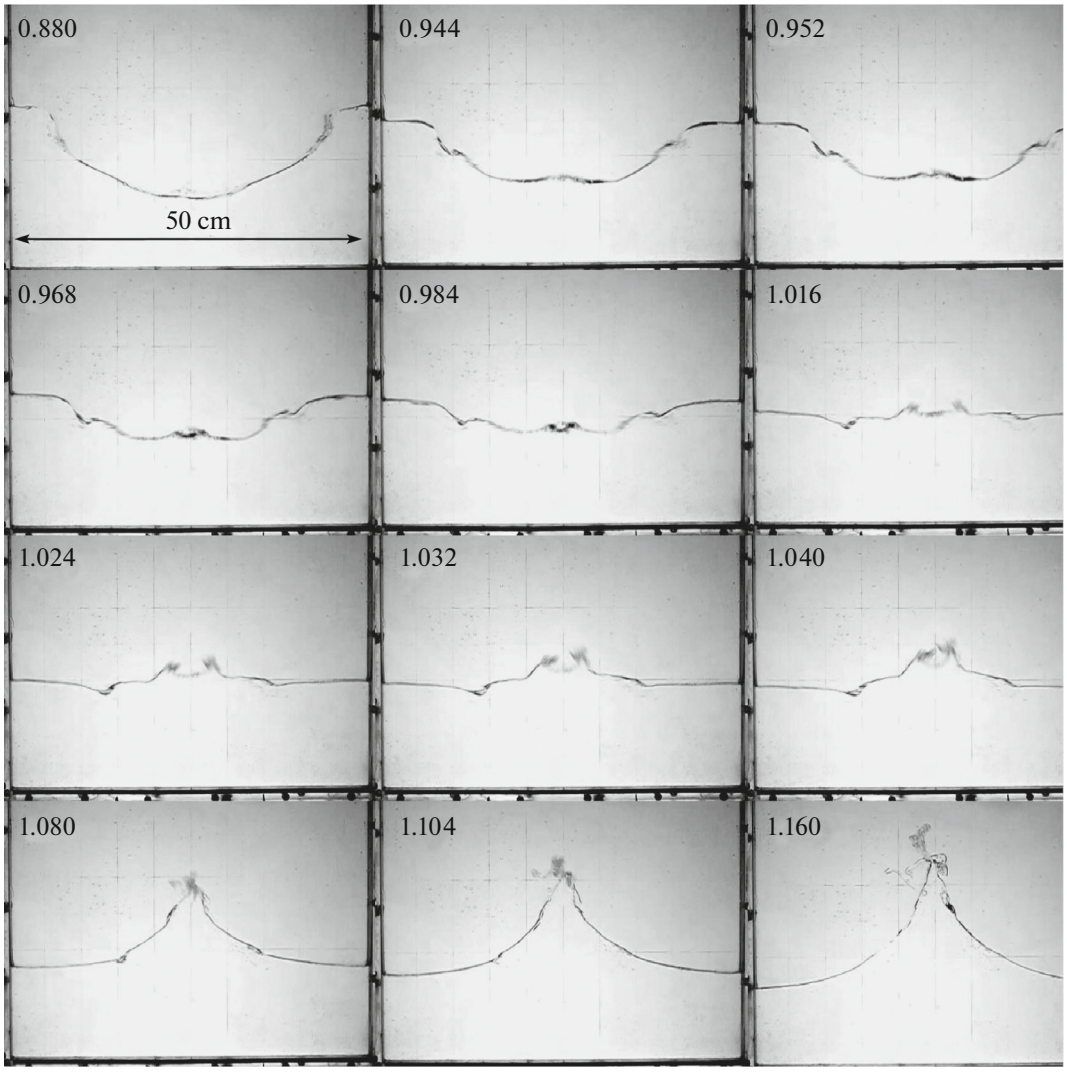

Fig. 10. Sequence of the video frames illustrating the process of collapse of the gravity Faraday waves on the free water surface during half the wave period: $\Omega = 21.67$ s^{-1} and $\Gamma \approx 0.30$; the instant of time is shown in the upper left corner of the frame.

viscosity and do not relate to the effect of the surface tension since its decrease (in the case of oil) or increase (in the case of sugar solution) with respect to its value for water does not affect the results obtained [12].

To interpret the experimental results obtained, we will use the following dispersion relation $\omega = \omega(k)$ obtained in [11] for the free standing gravity waves on the surface of infinitely deep viscous fluid which establishes the relation between the wave length λ, frequency ω, and damping coefficient b:

$$[1 + \zeta^2]^2 = 16\vartheta^3(\zeta - \vartheta), \tag{2.2}$$

where $\vartheta = \nu k^2/\omega_0$, $\zeta = -(\omega^* - 2\nu k^2)/\omega_0$, $\omega^* = b + i\omega$, $\omega_0 = (gk)^{1/2}$, $k = \pi n/L$, and $n = 2$.

In Fig. 12 we have reproduced the results of the numerical analysis of Eq. (2.2) in the form of the dependences $\omega(\lambda)$ and $b(\lambda)$. The frequency of free standing gravity waves on the surface of infinitely deep ideal fluid ($\nu = 0$) is determined by the relation $\omega_0 = (gk)^{1/2}$ and increases to infinity as the wave length decreases (data (*1*) in Fig. 12a). If the viscosity of oscillating fluid is taken into account, then the wave frequency takes zero value $\omega = 0$ at a certain critical wave length λ_{cr}. For water (*2*) this quantity is equal to $\lambda_{cr} = 0.02$ cm. As the viscosity increases to $\nu = 16.24$ cSt (aqueous sugar solution), we have $\lambda_{cr} = 0.15$ cm (data (*3*)). For vegetable oil (*4*) and 63% sugar solution (*5*) the critical wave lengths are estimated as $\lambda_{cr} = 0.40$ and 0.48 cm, respectively.

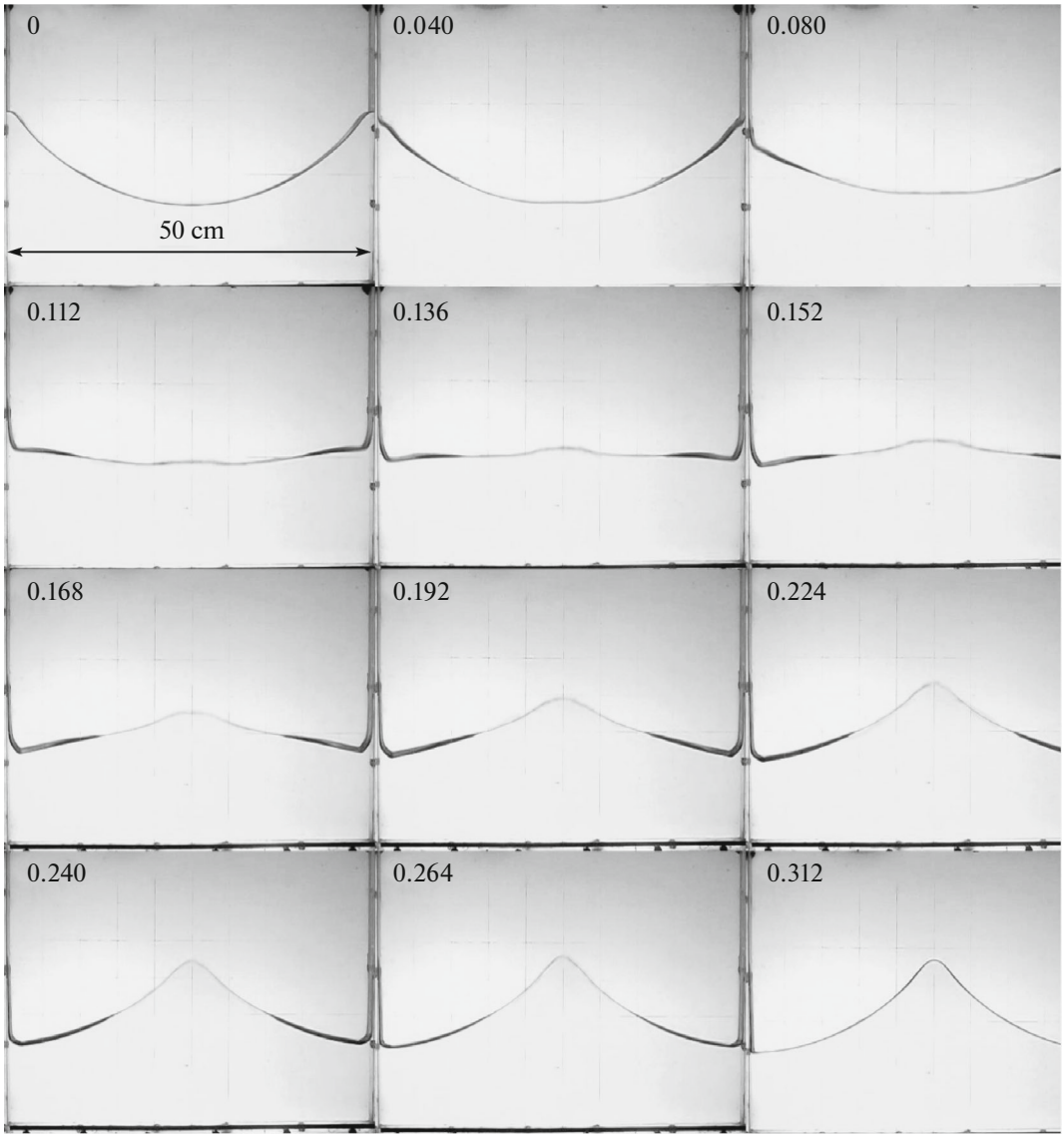

Fig. 11. Sequence of the video frames demonstrating the second wave mode on the surface of vegetable oil ($\nu = 63.34$ cSt) during half the wave period: $\Omega = 19.88\ \mathrm{s}^{-1}$ and $\Gamma = 0.30$.

Consequently, there are critical values of the wave length λ_{cr} which establish the shortwave limit of gravity wave excitation. When $\lambda < \lambda_{cr}$ the fluid viscosity suppresses completely any wave motion. An increase in the viscosity leads to an increase in this limit. This result confirms the experimental data on viscous regularization of breaking standing waves and makes it possible to explain the absence of small-scale perturbations on the wave profiles of viscous fluid by means of shortwave cutoff. Underestimated (as compared with the experiment) calculated values of λ_{cr} can be explained by the fact that both finite fluid depth and viscous losses on the lateral vessel walls and bottom are neglected in the dispersion relation (2.2).

In Fig. 12b we have reproduced the graphs of the damping coefficient as a function of the wavelength obtained in the numerical solution of (2.2) for water (*2*) and oil (*4*). For these fluids we have 0.0003 and 0.0193 s^{-1}, respectively, for the second wave mode ($\lambda = 50$ cm). The calculated values of the damping coefficient are significantly smaller than the experimental values (Table 2).

We will now estimate the contribution of viscous losses on the vessel walls. In [16, 17] it was shown that the damping coefficient b of a standing wave on the surface of fluid of depth h in the vessel of length L and width W can be determined as follows:

$$b = b_1 + b_2 + b_3,$$

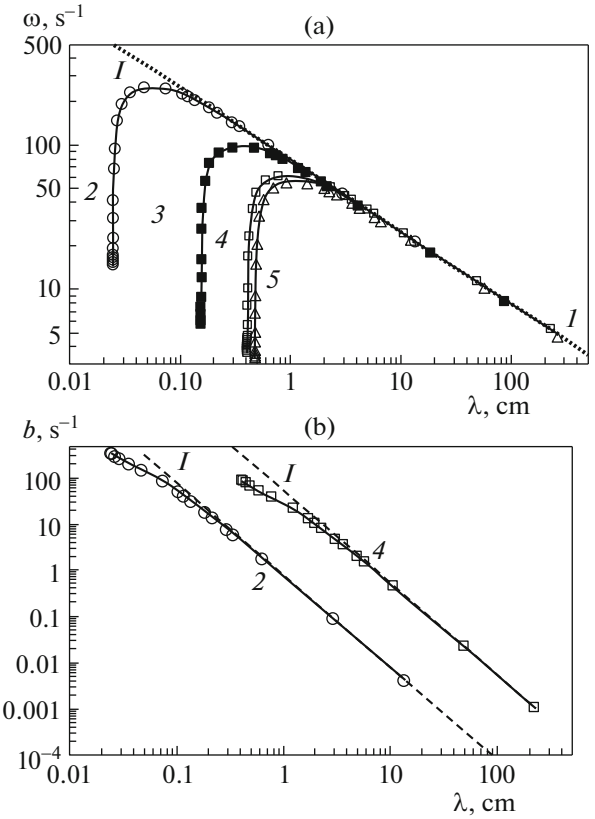

Fig. 12. Dependences $\omega(\lambda)$ and $b(\lambda)$ (a and b, respectively): *1–5* correspond to $\nu = 0,\ 1,\ 16.24,\ 63.34$, and 85.97 cSt, respectively.

$$b_1 = 2\nu k^2, \quad b_2 = \sqrt{\frac{\omega\nu}{2}}\left(\frac{L+W}{LW} + k\frac{L-2h}{L\sinh 2kh}\right), \quad b_3 = \sqrt{\frac{\omega\nu}{2}}k\frac{1}{\sinh 2kh}.$$

Here, the coefficients b_1, b_2, and b_3 determine the wave energy dissipation over the entire fluid volume, on the vessel walls, and on the bottom, respectively. In Table 2 we have given the measured (experimental) and calculated (theoretical) damping coefficients b_{exp} and b_{the}, as well as the values of b_{1-3}. Despite a certain difference between the experimental and theoretical values of the damping coefficient, we can see that dissipation on the vessel walls and bottom makes the main contribution to the wave energy losses while the losses in the fluid volume are rather small.

The estimate of the damping coefficient $\text{Re}[\omega^*] = b$ obtained from the dispersion relation (2.2) coincides with b_1 for water and oil. In Fig. 12b we have plotted the graphs of b_1 as a function of λ for water and oil (broken curves I).

Taking the surface tension of fluids σ into account and consideration of the capillary-gravity waves for which $\omega_0 = (gk + \sigma k^3/\rho)^{1/2}$ do not change [8, 9] the form of the dispersion relation (2.2). In this

Table 2

	Water, $\nu = 1$ cSt	Oil, $\nu = 63.34$ cSt	Sugar solution, $\nu = 85.97$ cSt
b_{exp}, s^{-1}	0.157	0.863	0.752
b_{the}, s^{-1}	0.065	0.525	0.632
b_1, s^{-1}	0.0003	0.0193	0.0275
b_2, s^{-1}	0.0634	0.4954	0.5916
b_3, s^{-1}	0.0013	0.0106	0.0126

case the values of the critical wave length for water, oil, and 63% sugar solution $\lambda_{cr} = 4.8 \times 10^{-6}$, 0.03, and 0.04 cm turn out to be significantly less than the corresponding quantities for the gravity waves.

Thus, although the dispersion relation (2.2) explains qualitatively the effect of viscous regularization of the wave motion for infinitely deep viscous fluid unbounded in the horizontal direction, it does not ensure quantitative coincidence with the experimental data since the effect of the finite fluid depth and the vessel walls is neglected in the theoretical model. Nevertheless, from (2.2) it follows that just the fluid viscosity ensures suppression of shortwave perturbations responsible for breaking the waves.

SUMMARY

As a result of the comprehensive experimental investigation of the standing gravity waves excited at parametric resonance, the quantitative data on the effect of fluid viscosity on the frequency range of excitement of the second wave mode, on the resonance dependences and the processes of damping and tending the oscillations to the steady-state regime.

It is found that increase in the kinematic fluid viscosity by 50 times as compared with water changes radically the dynamics of wave motion, namely, regularization of waves with total suppression of the process of their breaking in the form of jet ejection from the crest and its subsequent disintegration is observed.

From the numerical analysis of the dispersion relation for free standing gravity waves on the surface of a viscous fluid there follows the presence of the shortwave limit of existence of waves of this type. In this case viscous dissipation becomes the dominant factor suppressing the shortwave perturbations responsible for breaking the Faraday waves.

The work was carried out on the theme of the State Program No. AAAA-A17-117021310375-7 and with partial support for V.A. Kalinichenko from the Russian Foundation for Basic Research (project No. 18-01-00116).

REFERENCES

1. R. A. Ibrahim, "Recent Advances in Physics of Fluid Parametric Sloshing and Related Problems," ASME. J. Fluids Eng. **137** (9), 090801–090801–52. doi:10.1115/1.4029544
2. V. V. Bolotin, "Fluid Motion in an Oscillating Reservoir," Prikl. Mat. Mekh. **20**(2), 293–294 (1956).
3. R. A. Ibrahim, *Liquid Sloshing Dynamics: Theory and Applications* (Cambridge Univ. Press, Cambridge, 2005).
4. V. A. Kalinichenko and S. Ya. Sekerzh-Zenkovich, "Breakdown of parametric fluid oscillations," Fluid Dynamics **45** (1), 113–120 (2010).
5. V. A. Kalinichenko, "Breaking of Faraday Waves and Jet Launch Formation," Fluid Dynamics **44** (4), 577–586 (2009).
6. G. I. Taylor, "An Experimental Study of Standing Waves," Proc. Roy. Soc. London. Ser. A **218** (1132), 44–59 (1953).
7. H. Bredmose, M. Brocchini, D. H. Peregrine, and L. Thais, "Experimental Investigation and Numerical Modelling of Steep Forced Water Waves," J. Fluid Mech. **490**, 217–249 (2003).
8. H. Lamb, *Hydrodynamics* (Cambridge University Press, Cambridge, 1932; Gostekhizdat, Moscow, Leningrad, 1947).
9. H. H. LeBlond and F. Mainardi, "The Viscous Damping of Capillary-Gravity Waves," Acta Mechanica **68** (3–4), 203–222 (1987).
10. Yu. V. Sanochkin, Viscosity Effect on Free Surface Waves in Fluids," Fluid Dynamics **35** (4), 599–604 (2000).
11. L. N. Sretenskii, "Waves on the Surface of a Viscous Fluid. Pt. 1," Tr. TsAGI 541, 1–34 (1941).
12. A. V. Bazilevskii, V. A. Kalinichenko, and A. N. Rozhkov, "Viscous Regularization of Breaking Faraday Waves," JETP Letters **107** (11), 684–689 (2018).
13. G. N. Mikishev and B. I. Rabinovich, *Dynamics of Thin-Walled Structures with Sections Containing Fluid* (Mashinostroenie, Moscow, 1971) [in Russian].
14. A. V. Bazilevskii, S. Wongwises, V. A. Kalinichenko, and S. Ya. Sekerzh-Zen'kovich, "Experimental Study of the Bottom Structure Effect on the Damping of Standing Surface Waves in a Rectangular Vessel," Fluid Dynamics **36** (4), 652–657 (2001).
15. S. V. Nesterov, "Parametric Excitation of Waves on the Surface of a Heavy Liquid," Morskie Gidrofiz. Issledovaniya 3 (45), 87–97 (1969).
16. G. H. Keulegan, "Energy Dissipation in Standing Waves in Rectangular Basins," J. Fluid. Mech. **6** (1), 33–50 (1959).
17. J. W. Miles, "Surface-Wave Damping in Closed Basins," Proc. R. Soc. Lond. A. **297**, 459–475 (1967).